Article

High-Frequency Oscillations in the Belousov#Zhabotinsky Reaction

Tama#s Ba#nsa#gi Jr., Marcin Leda, Masahiro Toiya, Anatol M. Zhabotinsky, and Irving R. Epstein

J. Phys. Chem. A, **2009**, 113 (19), 5644-5648• Publication Date (Web): 17 April 2009

High-Frequency Oscillations in the Belousov−Zhabotinsky Reaction

Tamás Bánsági, Jr., Marcin Leda, Masahiro Toiya, Anatol M. Zhabotinsky,† and Irving R. Epstein*

Department of Chemistry and Volen Center for Complex Systems, MS 015, Brandeis University, Waltham, Massachusetts 02454-9110

Received: February 12, 2009; Revised Manuscript Received: March 17, 2009

Chemical oscillations in the classic Belousov−Zhabotinsky (BZ) system typically have a period of a few minutes, which can be increased significantly by changing the organic substrate. Here we show that by changing the temperature and concentrations, an increase of 3−4 orders of magnitude in the *frequency* of BZ oscillations can be obtained. At elevated temperatures, in high concentration mixtures, the cerium-catalyzed reaction exhibits sinusoidal oscillations with frequencies of 10 Hz or greater. We report the effect of temperature on the frequency and shape of oscillations in experiments under batch conditions and in a four-variable model. We show that our simple model accurately captures the complex temporal behavior of the system and suggests paths toward even higher frequencies.

Introduction

The Belousov−Zhabotinsky (BZ) reaction[1,2] continues to draw considerable scientific interest even five decades after its discovery. Over the years, the name has come to refer to a family of metal-ion-catalyzed, bromate-driven reactions in which organic substrates in acidic media are oxidized to give oscillations in the concentrations of various intermediates. The detailed mechanism of the classical, cerium-ion-catalyzed reaction system was first described by Field, Körös, and Noyes[3] (FKN). By reducing its complexity to a few coupled elementary pseudoreactions, Field and Noyes were able to construct a simplified mathematical model,[4] now known as the Oregonator, which exhibits oscillatory limit cycles. The model also successfully describes a wealth of complex phenomena seen in the BZ reaction, both temporal, such as excitability,[5,6] bistability,[7] stirring effects,[8,9] quasiperiodicity, and chaos,[10,11] and spatial, including traveling waves,[12] target and spiral patterns,[13,14] scroll rings,[15] and their orientation dynamics in advective fields.[16]

The Oregonator has been also used to model the effect of temperature on oscillations, prompted by Körös' experimental study[17] of the BZ reaction between 15 and 35 °C with Ce^{3+}, Mn^{2+}, and $Ru(bipy)_3^{2+}$ as catalysts. He pointed out that the complex BZ system behaves, in a sense, as if there is a single rate-determining step, since it obeys the Arrhenius equation, yielding practically the same activation energy for all three catalysts. In addition to experimentally confirming these striking findings, Blandamer et al.,[18,19] by systematically varying the rate constants in the model, identified the model step that most influences the frequency as the one representing the reaction between bromide and bromate ions to yield bromous acid. Misra[20] studied the BZ reaction both experimentally and numerically over a significantly wider temperature regime, from 30 to 90 °C, in a continuous-flow stirred tank reactor (CSTR). By using an extended Oregonator model that incorporates the bromination of malonic acid by hypobromous acid and bromine and the oxidation of malonic acid and its brominated derivatives by Ce^{4+} and other species to form bromide and free radicals, he demonstrated that the frequency cannot continue to grow exponentially without limit. Instead, with increasing temperature, oscillations disappear at a critical temperature via a Hopf bifurcation. Over this same range of temperatures, the amplitude of oscillations, however, remains essentially unchanged before quickly dropping near the bifurcation point. Similar conclusions were drawn by Strizhak and Didenko[21] for temperatures below 33 °C, employing the kinetic scheme of Györgyi and Field.[22]

None of the studies above, regardless of the model or scheme employed, examined the effects of varying the acidity or how the shape of the oscillations varies with temperature. Concentrations of reactants, except for sulfuric acid, were typically maintained in the range explored in the prior literature for the BZ reaction. Although increases in temperature did, as expected, shorten the period from typical values of ∼5 min to as low as 2 s,[20] one may wonder what range of frequencies is accessible to the BZ reaction. Use of alkylated species,[23,24] such as methylmalonic acid, or aromatic species,[25] such as pyrocatechol, as the substrate can lengthen the period by a factor of 10 or more. Might it be possible to *decrease* the period by several orders of magnitude, and could one model such high-frequency oscillations within the Oregonator framework? Here, we seek to answer these questions by exploring the uncharted regime of higher concentrations and temperatures, aiming to find high-frequency oscillations and to numerically reproduce, with a high degree of accuracy, the temperature dependence of the frequency and amplitude as well as the shape of oscillations with a four-variable Oregonator model. We also use the model to roam the reaction's phase space in search of even higher frequency oscillations in this well-studied chemical system.

Experimental Section

Oscillatory profiles are obtained by electrochemical measurements within the temperature range of 40−80 °C. Reaction mixtures are prepared from aqueous stock solutions of analytical-grade sodium bromate ($NaBrO_3$, Fisher), malonic acid ($CH_2(COOH)_2$, Sigma-Aldrich), sulfuric acid (H_2SO_4, Fisher, 5 M), and ceric ammonium nitrate ($(NH_4)_2Ce(NO_3)_6$, Fisher). The initial concentrations are $[NaBrO_3] = 0.5$ M, $[CH_2-$

* To whom correspondence should be addressed.
† Deceased, September 16, 2008. This paper is dedicated to the memory of Professor Anatol M. Zhabotinsky.

10.1021/jp901318z CCC: $40.75
Published on Web 04/17/2009

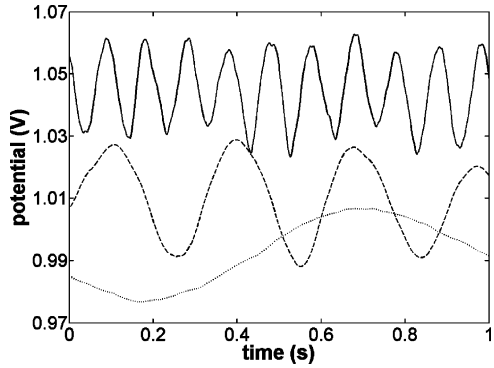

Figure 1. Oscillatory traces at three temperatures in the BZ reaction: 40 (dotted), 60 (dashed), and 80 °C (solid). Initial conditions are given in the Experimental Section. Profiles are shifted along the abscissa for clarity.

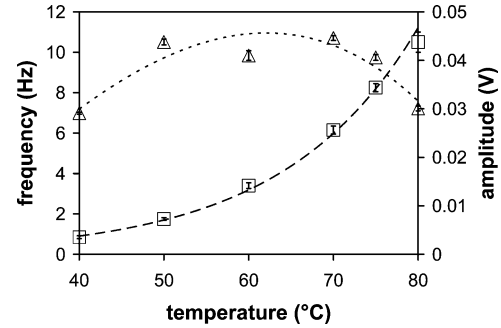

Figure 2. Initial oscillatory frequencies (squares) and amplitudes (triangles) in the temperature range 40−80 °C. Dashed line represents exponential curve fitted to experimental frequency data. Dotted line corresponds to the cubic curve drawn to aid the eye. Reactant concentrations are listed in the Experimental Section.

$(COOH)_2]$ = 2.0 M, $[H_2SO_4]$ = 1.5 M, $[(NH_4)_2Ce(NO_3)_6]$ = 1.0 mM, except where otherwise specified.

As the working electrode we use a glass-coated platinum wire with one end open to the electrolyte, immersed in 0.25 mL of BZ mixture held in a thin-walled 5 mm diameter glass tube. The working electrode potential is measured against a saturated calomel electrode (SCE, Fisher Scientific Accumet, gel filled) placed in a 1.5 cm diameter glass tube containing 0.25 M sodium sulfate (Na_2SO_4, Fisher) solution. Both half cells are submerged in a thermostat (Techne equipped with Techne TE-10D digital immersion circulator) and connected through a salt bridge, a 1 mm diameter glass U-tube filled with 0.25 M sodium sulfate in an agar−gel matrix (melting point ≈ 85 °C). Reaction mixtures are stirred with a 0.8 mm diameter glass rod attached to a high-rpm drill (Dremel 300). The potential difference is recorded with a high-performance USB acquisition module (Data Translation 9812) at sampling frequencies ranging from 100 to 1000 Hz. Despite the significant heat production, working with such small volumes of reaction mixture in the arrangement described above enables us to reliably keep the temperature within a ±1 °C range around its target value in the BZ half cell. Evaporation is negligible, as there is no discernible change in the height of the menisci, even at 80 °C. We are able to resolve oscillations with amplitudes of 10 mV and higher.

After lowering the fully assembled electrochemical cell into the water bath of the thermostat, we inject the requisite amounts of all preconditioned reagents, except the catalyst, into the BZ-batch half cell. Subsequently, under vigorous stirring, we add the catalyst to start the reaction.

Experimental Results

The preoscillatory induction period decreases with temperature, from about 300 s at 40 °C to about 30 s at 80 °C. During this portion of the reaction, the potential gradually decreases from its initial maximum value. This downward drift of the average potential continues throughout the oscillations and beyond, until the half-cell potential difference reaches zero. This effect can, however, be neglected within sufficiently short intervals.

Typical oscillatory profiles at several temperatures are shown in Figure 1. For better comparison, each is displaced along the time axis to fit within a 1 s interval. The profiles reveal the strong temperature dependence of the oscillatory frequency. The waveform is nearly sinusoidal between 40 and 80 °C, in contrast to the relaxation oscillations observed closer to room temperature. The data also show a small decrease in amplitude over the given temperature range.

In all cases, as the reaction proceeds, the frequency gradually decreases until oscillations finally cease with a period 20−30% longer than at the start. The number of cycles lessens with increasing temperature and drops to about 15 at 80 °C. The relative position of the curves along the ordinate suggests that the average potential rises with increasing temperature, though this conclusion is somewhat uncertain owing to small variations (<50 mV) from experiment to experiment in the overall potential differences between the BZ and SCE half cells.

Initial oscillatory frequencies and amplitudes for temperatures between 40 and 80 °C are presented in Figure 2. The frequency grows exponentially with temperature over the studied range, while the amplitude peaks at about 65 °C. The calculated activation energy is 58.0 ± 0.7 kJ/mol, in good agreement with previous studies.[17,19,26]

We also carried out experiments with 1,4-cyclohexanedione (CHD) as the organic substrate. In this set of experiments, ferroin is used as the catalyst and the traces are acquired spectrophotometrically. The maximum frequency of sinusoidal oscillations is measured to be 12 Hz with $[CHD]_0$ = 0.6 M, $[NaBrO_3]_0$ = 0.4 M, $[H_2SO_4]_0$ = 2.0 M, and [Ferroin] = 0.5 mM at 85 °C. We note that under such conditions we see surprisingly vigorous gas production in this reaction,[27] which is often regarded as a bubble-free BZ variant.

Model

The numerical analysis is based on a model incorporating all reactant species proposed by Zhabotinsky et al.[28] to describe the shape of oscillations and wave properties in the BZ reaction. The simplified set of equations used to describe our experimental findings is

$$dX/dt = -k_2h_0XY + k_3h_0AY - 2k_4'X^2 - k_5h_0AX + k_{-5}U^2 + k_6U(C-Z) - k_{-6}XZ \quad (1)$$

$$dY/dt = -k_2h_0XY - k_3h_0AY + qk_7BZ + k_9B \quad (2)$$

$$dZ/dt = k_6U(C-Z) - k_{-6}XZ - k_7BZ \quad (3)$$

$$dU/dt = 2k_5h_0AX - 2k_{-5}U^2 - k_6U(C-Z) + k_{-6}XZ \quad (4)$$

where $X = [HBrO_2]$, $Y = [Br^-]$, $Z = [Ce^{4+}]$, $U = [HBrO_2]$, h_0 is Hammet's acidity function,[29] $A = [NaBrO_3] = h_0/(0.2 + h_0)[NaBrO_3]_0$, $B = [MA]$, $C = [Ce^{3+}] + [Ce^{4+}]$, and $k_4' = k_4(1 + 0.87h_0)$. For numerical calculations, based on the initial reactant concentrations, we assign A_0 = 0.5 M, B_0 = 2 M, C = 0.001 M, and h_0 = 3, which corresponds to $[H_2SO_4]$ = 1.5 M. The

TABLE 1: Rate Parameters[a]

rate constant	20 °C	40 °C	ΔG [kJ/mol]	A[b]	80 °C	80 °C (this paper)
k_2 [M^{-2} s^{-1}]	7.57×10^6	1.2×10^7	15.0	1.24×10^7	2.60×10^7	4.95×10^7
k_3 [M^{-1} s^{-1}]	2.0	15	74.3	1.20×10^{11}	430	81.7
k_4 [M^{-2} s^{-1}]	8.6×10^3	1×10^4	3.23	111	1.3×10^4	2.5×10^4
k_5 [M^{-2} s^{-1}]	10	60	65.8	1.83×10^{10}	1187	3158
k_{-5} [M^{-1} s^{-1}]	4.2×10^6	6×10^6	11.1	1.35×10^6	1.1×10^7	2.1×10^7
k_6 [M^{-1} s^{-1}]	5×10^4	9×10^4	19.9	6.00×10^5	2.4×10^5	4.6×10^5
k_{-6} [M^{-1} s^{-1}]	5×10^4	2×10^4	5.99	798	3.7×10^4	6.95×10^4
k_7 [M^{-1} s^{-1}]	0.4	0.8	23.9	25.0	2.56	30.5
k_9 [s^{-1}]	3.3×10^{-6}	5×10^{-6}	13.3	2.67×10^{-6}	1.0×10^{-5}	2.4×10^{-5}

[a] Values in columns 2 and 3 are taken from ref 28. Values of the energy of activation ΔG in column 4 and the pre-exponential factor A in column 5 are computed from values of the rate constants in columns 2 and 3. Values in column 6 are obtained by extrapolation using values from columns 2 and 3. In column 7, values are adjusted to experiments at 80 °C. [b] Units are same as those for k_i.

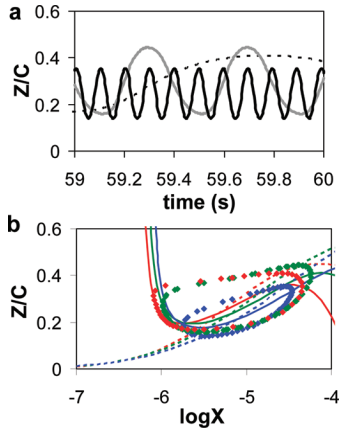

Figure 3. (a) Oscillatory solutions to systems 1−4 at $T = 80$ (black), 60 (gray), and 40 °C (dotted). $A_0 = 0.5$ M, $B = 2$ M, $h_0 = 3$ M, and $C = 0.001$ M. (b) Projections of limit cycles (composed of circles) on phase plane log X vs Z/C for temperatures $T = 80$ (blue), 60 (green), and 40 °C (red). Time elapsed between consecutive symbols: 5 ms. Solid and dashed lines are zero-growth isoclines (nullclines) for X and Z, respectively, calculated for the three temperatures. Note that the abscissa is logarithmic.

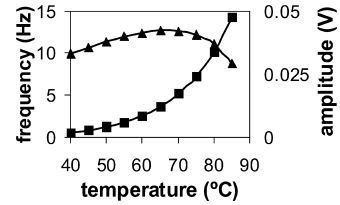

Figure 4. Simulated dependences of frequency (squares) and amplitude (triangles) of potential oscillations on temperature. Amplitude is calculated as $RT/F[\ln(Z_{max}/(C - Z_{max})) - \ln(Z_{min}/(C - Z_{min}))]$, where F is Faraday's constant. Parameter values are the same as in Figure 3.

stoichiometric parameter q is set to 0.6 in accordance with ref 28.

Numerical Results

Modeling our experimental findings requires rate constants applicable at high temperatures. For the reactions that lead to eqs 1−4, however, these quantities are available[28] only for 20 and 40 °C (Table 1, columns 2 and 3). To estimate their values at higher temperatures, we can use the absolute rate theory, according to the which a rate constant can be calculated as $k(T) = AT \exp(-E_a/RT)$, where k, A, T, and E_a are the rate constant, pre-exponential factor, absolute temperature, and activation energy, respectively. For the rate constant values given by this formula (listed in column 6 of Table 1), oscillations vanish at temperatures as low as 55 °C with frequencies below 1 Hz at the Hopf bifurcation. In our experiments, however, we observe oscillations at 60 °C (~3 Hz) and higher temperatures.

To address this discrepancy and to quantitatively capture the experimentally observed oscillations, we adjusted all rate constants to obtain the best fit with the experimental data, specifically the frequency and amplitude of oscillations at 80 °C for $A_0 = 0.5$ M, $B_0 = 2$ M, $C = 0.001$ M, and $h_0 = 3$ and the concentration of bromate A_0 at which the Hopf bifurcations at 40 and 60 °C occur for $B_0 = 2$ M, $C = 0.001$ M, and $h_0 = 3$ (Figure 5a). We chose the bromate vs temperature phase diagram (Figure 5a) because the system is quite sensitive to changes in the bromate concentration. We believe that this approach is more reliable than simply fitting potential time series because the fast oscillations last only a few seconds.

Comparing the resulting constants (column 7) to their counterparts given by the absolute rate theory (column 6), we find that only the differences in the k_3 and k_7 values (rows 3 and 9) are significant. These steps correspond, respectively, to the following reactions

$$H^+ + Br^- + HBrO_3 \leftrightarrow HBrO_2 + HOBr \quad (5)$$

$$Ce^{4+} + CHBr(COOH)_2 \leftrightarrow Ce^{3+} + CBr(COOH)_2^{\bullet} + H^+ \quad (6)$$

Reaction 5 was identified by Blandamer at al.[19] as the major determinant of the oscillatory frequency, and its activation energy was measured to be 54 kJ/mol.[30] Substituting this value and the corresponding rate constant at 20 °C (Column 2) into the absolute rate theory equation yields a rate constant of 86.6 M^{-1} s^{-1} at 80 °C, which is in excellent agreement with that calculated in this study. The activation energy of reaction 6 is reported to be 67 kJ/mol[21] and is assumed to be close to the total energy of activation,[31] which is 58 kJ/mol. With the extrapolation method, these two values of E_a both yield fairly good estimates for k_7, 42.9 and 22.9 M^{-1} s^{-1}, respectively. Hence, we conclude that our corrections for constants k_3 and k_7 are reasonable and consistent with literature data.

With these adjustments to the rate constants, the calculated frequencies, amplitudes, and shapes of the oscillatory profiles faithfully reflect our experimental findings (see Figure 3a). Analyzing the dynamics of the four-variable model on the phase plane provides detailed insights into the behavior of the BZ reaction at elevated temperatures. According to Figure 3b, the limit cycle is fairly symmetric for all three temperatures, which is consistent with the sinusoidal character of the oscillatory traces. As the temperature is increased, the limit cycle shrinks and the oscillations become substantially faster. The distance

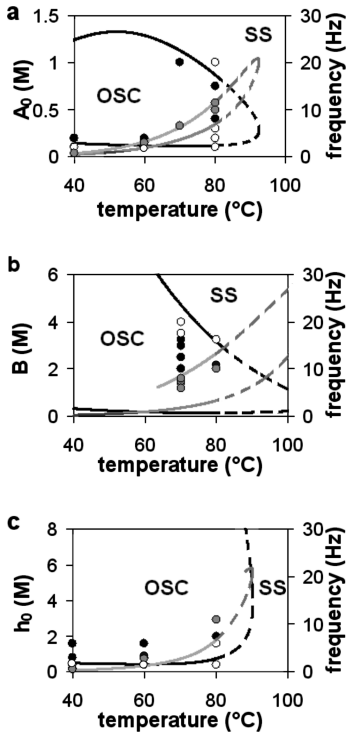

Figure 5. Calculated parametric diagrams $T-A_0$ (a), $T-B$ (b), and $T-h_0$ (c). Remaining parameters are the same as in Figure 1. Black lines indicate boundaries between dynamic states. Symbols OSC and SS denote areas corresponding to oscillation and stationary states, respectively. The secondary ordinate axis shows the oscillation frequency (gray lines) at Hopf bifurcation points. Circles correspond to experimental results: no oscillations (empty circles), oscillations (solid back circles), with frequencies shown by solid gray circles.

between the extrema of Z, however, changes much less rapidly, which translates to oscillations with nearly constant amplitude throughout the studied temperature regime, as observed in experiment and previously reported for dilute BZ mixtures.[20]

The oscillatory frequency and amplitude dependence on temperature obtained from the model are presented in Figure 4. As in the experiments, there is an exponential relationship between frequency and temperature. The calculated amplitude exhibits the same tendencies seen in the experiments (Figure 2). Compared to the frequency, the amplitude remains within a narrow range, first growing, then passing through a maximum, and finally decreasing as the temperature approaches 80 °C. Simulations suggest that the sharp fall in amplitude continues while the frequency rapidly increases until oscillations finally disappear around 90 °C with a frequency of about 20 Hz. Spectrophotometric measurements at higher temperatures with ferroin as catalyst using slightly different reactant concentrations support this prediction. The oscillatory regime in these ferroin-catalyzed experiments extends above 80 °C, and the frequency can reach as high as 18 Hz for temperatures near 100 °C.

The fitted total activation energy is 68.2 ± 0.1 kJ/mol, which exceeds that found in experiment. This difference is a consequence of the tendency of the model to underestimate frequencies for lower temperatures, as it is primarily designed to accurately describe the high-frequency oscillations.

Our model, despite the aforementioned weakness, enables us to numerically explore the high-frequency oscillatory regime of the BZ system. When mapping this domain of the reaction's phase space, we keep all but one parameter as well as the total catalyst concentration constant while systematically changing the remaining parameter and the temperature. Guided by the numerical results, we carry out experiments along sections of the calculated boundaries separating oscillatory and stationary regimes to test the model over a broader domain in the phase space. The resulting parametric diagrams (see Figure 5) demonstrate that our model largely reflects the empirical findings. Boundaries and frequencies are in good agreement with the experimental data, though in a few cases, typically at high temperatures, the oscillatory domains are narrower than predicted by the model. This discrepancy may result, at least in part, from the sharp drop in amplitude that occurs near the Hopf bifurcation, which leads to oscillations that we cannot resolve experimentally. Simplifications in the model that reduce the complexity of the system may also lead to quantitative mismatches between experiment and simulation. The approximate calculation of hydronium ion concentrations, especially at high temperatures, is another factor likely to reduce the accuracy of the model. Looking at Figure 5, however, we conclude that the four-variable model renders all dynamical aspects of the high-temperature reaction rather well. Consequently, we can make calculations with some confidence up to 100 °C to further explore the phase space. The dashed lines show the likely characteristics of the reaction at temperatures near the normal boiling point of water. It seems probable that, by decreasing the malonic acid concentration while keeping the others constant, one could reach ~25 Hz oscillations near 100 °C.

Conclusions

Our experimental results show that chemical systems such as the Belousov−Zhabotinsky reaction can support oscillations with frequencies above 10 Hz. We demonstrated that this frequency regime is easily accessible and studying it requires no special equipment. High-frequency oscillations can, however, be sustained only for a few seconds in closed systems, though they should continue indefinitely in a flow reactor.

Numerical simulations show that our four-variable model quantitatively describes all dynamical features of the reaction between 40 and 80 °C. This allowed us to map the phase space at higher temperatures and identify possible pathways leading to frequencies approaching 25 Hz. These experiments would require a sealed tube to avoid evaporation, a stir bar instead of a glass rod immersed in the reaction mixture from above, and perhaps a high-performance temperature control system able to compensate for the rapid heat production.

In a high-pressure environment, it might be possible to exceed significantly even the 3−4 orders of magnitude increase we achieved here over the typical BZ oscillation frequency. In principle, the temperature could be increased to the critical point of water (374 °C) while maintaining oscillations, though other factors, including the increased dissociation of water and the decarboxylation of malonic acid, would have to be taken into account. It would perhaps be worthwhile to make calculations using our model to estimate a feasible frequency limit that could be reached experimentally if one were interested in increasing the speed of chemical computation devices[32] that incorporate BZ oscillators.

Acknowledgment. We thank the National Science Foundation (grant CHE-0615507) and the Defense Advanced Research Projects Agency for support.

References and Notes

(1) Belousov, B. P. *Sb. Ref. Radiats. Med.*; Medgiz: Moscow, 1958; p 145.

(2) Zhabotinsky, A. M. *Biofizika* **1964**, *9*, 306.
(3) Field, R. J.; Körös, E.; Noyes, R. M. *J. Am. Chem. Soc.* **1972**, *94*, 8649.
(4) Field, R. J.; Noyes, R. M. *J. Chem. Phys.* **1974**, *60*, 1877.
(5) Field, R. J.; Noyes, R. M. *Faraday Symp. Chem. Soc.* **1974**, *9*, 21.
(6) Ruoff, P. *Chem. Phys. Lett.* **1982**, *72*, 76.
(7) Geiseler, W.; Föllner, H. H. *Biophys. Chem.* **1977**, *6*, 107.
(8) Ruoff, P. *J. Phys. Chem.* **1993**, *97*, 6405.
(9) Epstein, I. R. *Nature (London)* **1995**, *374*, 321.
(10) Richetti, P.; Roux, J. C.; Argoul, F.; Arneodo, A. *J. Chem. Phys.* **1987**, *86*, 3339.
(11) Argoul, F.; Arneodo, A.; Richetti, P.; Roux, J. C.; Swinney, H. L. *Acc. Chem. Res.* **1987**, *20*, 436.
(12) Armstrong, G. R.; Taylor, A.; Scott, S. K.; Gáspár, V. *Phys. Chem. Chem. Phys.* **2004**, *6*, 4677.
(13) Zaikin, A. N.; Zhabotinsky, A. M. *Nature (London)* **1970**, *225*, 535.
(14) Winfree, A. T. *Science* **1972**, *175*, 634.
(15) Alonso, S.; Sagués, F.; Mikhailov, A. S. *J. Phys. Chem. A* **2006**, *110*, 12063.
(16) Luengviriya, C.; Hauser, M. J. B. *Phys. Rev. E* **2008**, *77*, 056214.
(17) Körös, E. *Nature (London)* **1974**, *251*, 703.
(18) Blandamer, M. J.; Morris, S. H. *J. Chem. Soc., Faraday Trans* **1975**, *I 71*, 2319.
(19) Blandamer, M. J.; Roberts, D. L. *J. Chem. Soc., Faraday Trans* **1977**, *73*, 1056.
(20) Misra, G. P. *Chem. Phys. Lett.* **1992**, *191*, 435.
(21) Strizhak, P. E.; Didenko, O. Z. *Theor. Exp. Chem.* **1997**, *33*, 133.
(22) Györgyi, L.; Field, R. J. *J. Phys. Chem.* **1991**, *95*, 6594.
(23) Ruoff, P.; Schwitters, B. *Z. Phys. Chem.-Wiesbaden* **1982**, *132*, 125.
(24) Chen, Y. F.; Lin, H. P.; Sun, S. S.; Jwo, J. J. *Int. J. Chem. Kinet.* **1996**, *28*, 345.
(25) Harati, M. Ph.D. thesis, University of Windsor, 2008.
(26) Nagy, G.; Körös, E.; Oftedal, N.; Tjelflaat, K.; Ruoff, P. *Chem. Phys. Lett.* **1996**, *250*, 255.
(27) Farage, V. J.; Janjic, D. *Chem. Phys. Lett.* **1982**, *88*, 301.
(28) Zhabotinsky, A. M.; Buchholtz, F.; Kiyatkin, A. B.; Epstein, I. R. *J. Phys. Chem.* **1993**, *97*, 7578.
(29) Hammett, L. P.; Deyrup, A. J. *J. Am. Chem. Soc.* **1932**, *54*, 2721.
(30) Kshirsagar, G.; Field, R. J. *J. Phys. Chem.* **1988**, *92*, 7074.
(31) Ruoff, P. *Physica D* **1995**, *84*, 204.
(32) Adamatzky, A. *Computing in Nonlinear Media and Automata Collectives*; IOP: London, 2001.

JP901318Z